

Internal structure of diamond nanocrystals by modeling and PDF analysis

S. Stelmakh^a, S. Gierlotka^a, K. Skrobas^a, W. Palosz^b, and B. Palosz^a

^aInstitute of High Pressure Physics, Poland, ^bBrimrose Corporation, Sparks, Md, USA
E-mail: svrit@unipress.waw.pl

Calculations

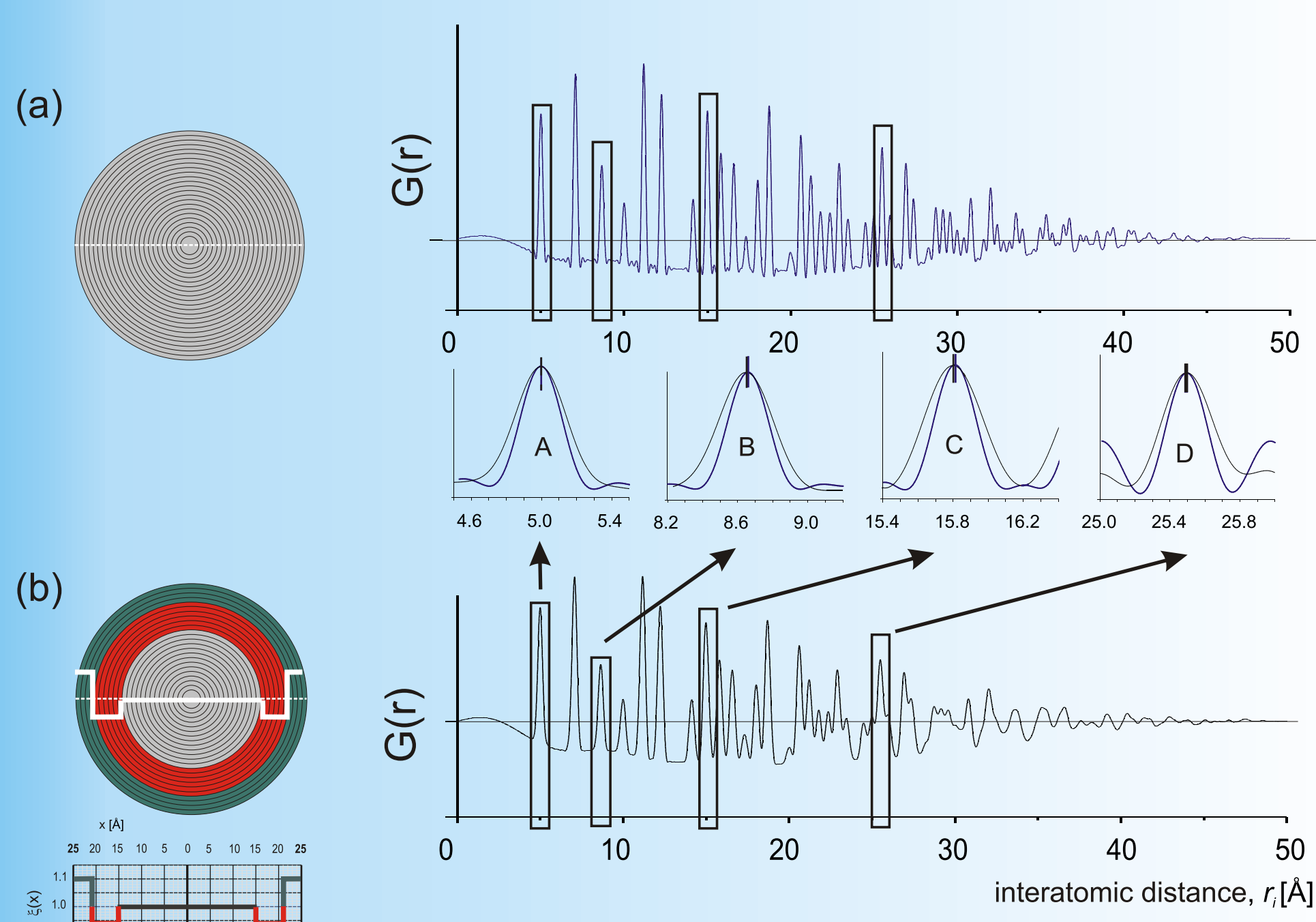


Fig. 1 Models of spherical 5 nm diamond nanograin with, (a), a perfect cubic lattice and, (b), the same grain modified by introduction of two spherical density waves, and their corresponding $G(r)$ functions.

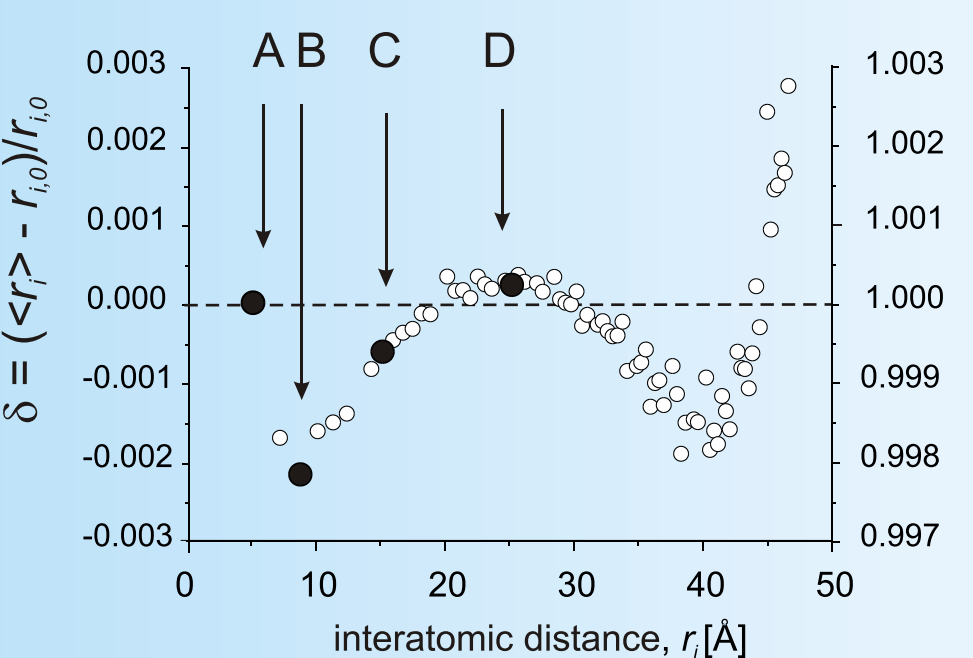


Fig. 2 Relative differences between inter-atomic distances in the grain with density modulation waves and those in the perfect diamond lattice; open circles present changes of all individual r -distances, full circles correspond to the distances marked in Fig. 1.

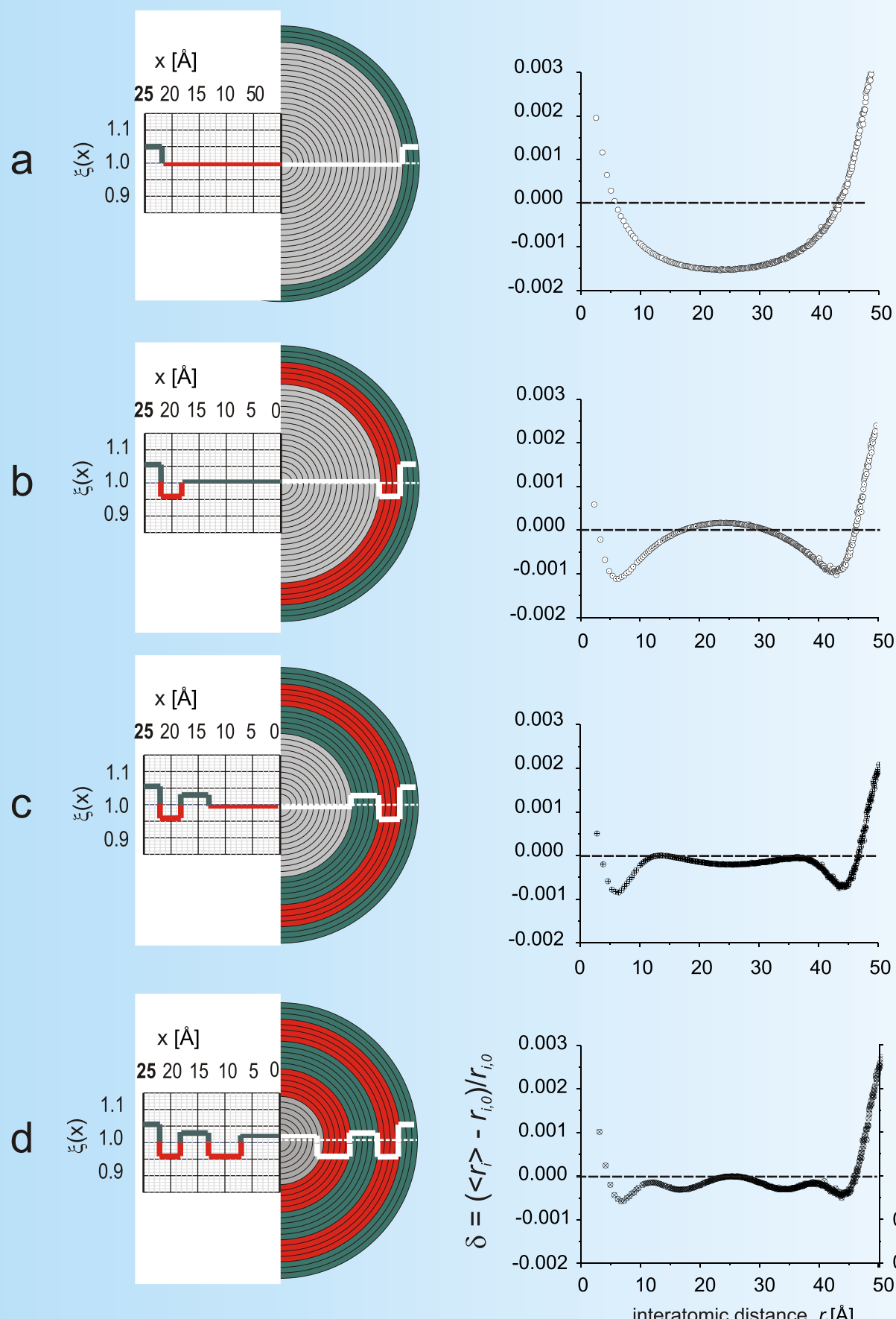


Fig.3 Theoretical d -plots calculated for 5 nm diamond models with up to 3 density waves between the grain core and the surface.

Experiment

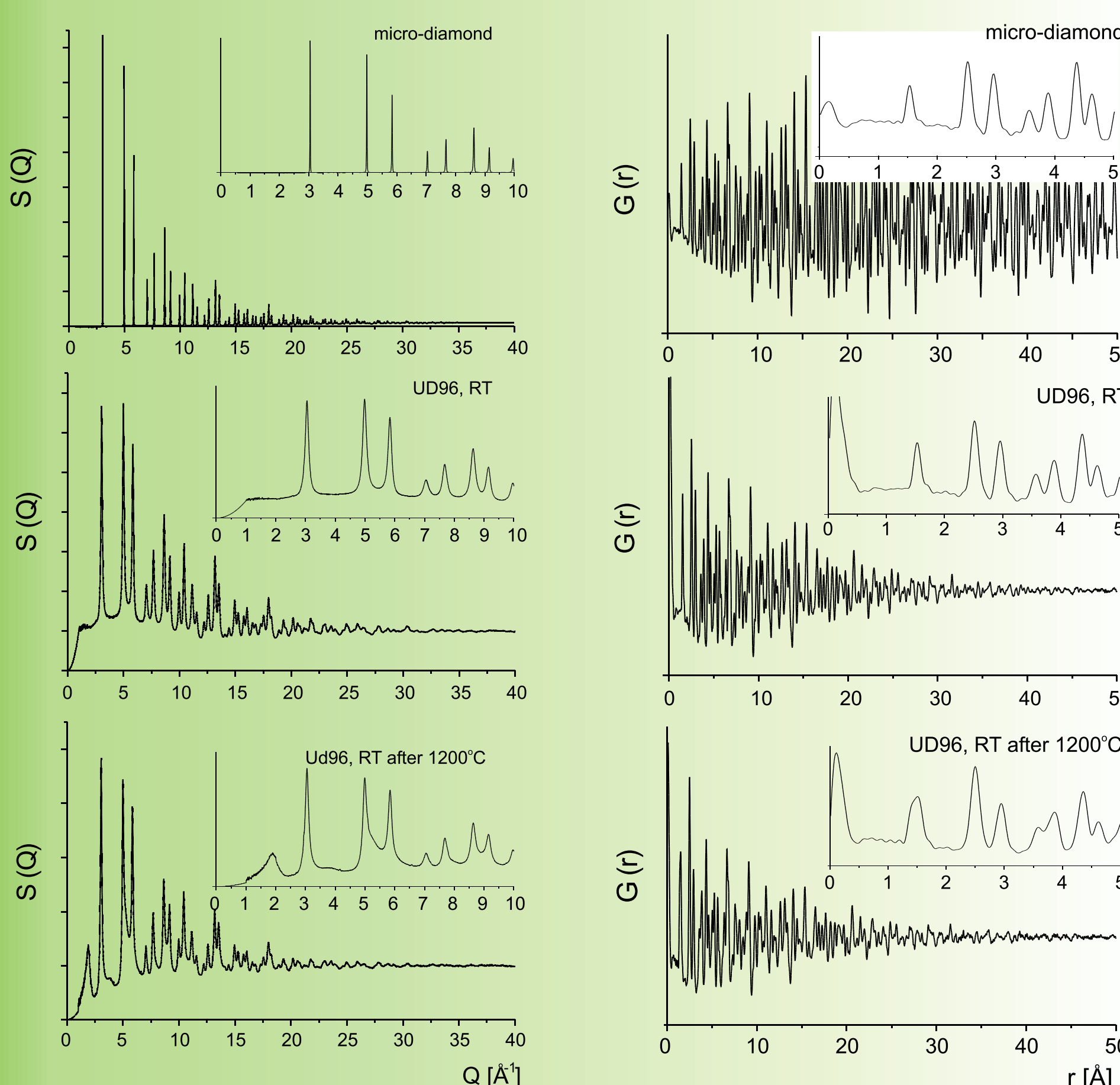


Fig.4 Experimental scattering factors of microdiamond, and UD96 powders as synthesized and annealed at 1200°C for 1 h.

Fig.5 Experimental $G(r)$ plots obtained for $S(Q)$ s of Fig. 5.

Abstract

The structure of nanocrystalline diamond was approximated by spherical nanograins assuming that the grain core (presumably with a perfect crystal lattice) is surrounded by a sequence of shells with (basically) the same atomic architecture as that in the bulk but with altered density. We call such a model a **nanocrystal with density modulation waves**.

To examine the effect of density modulation present in nanograins, we built atomistic models of nanograins and compared the average values of inter-atomic distances calculated for the grains with density waves to those of the parent perfect crystal lattice.

Background/theoretical

The model

Density modulation, if present in a real nanocrystal, should be describable by a continuous function. Experimentally, however, it is impossible to determine the exact shape of such a function. For the sake of simplicity we decided to approximate the actual modulation by a sequence of discrete changes in the material density.

To build a model with density modulation waves, the space within the volume of a spherical grain was subdivided into shells, each shell being defined as a space between two concentric spherical surfaces. Each shell has its own density (determined by inter-atomic distances in the shell). A set of adjacent shells can form a density modulation which we call "the wave". We specify "borders" of each density modulation wave, i.e. we define the smallest and largest radii of the set of shells forming a given density modulation wave, the sign (extended, "+", or shrunk, "-", inter-atomic distances relative to the starting perfect lattice), and magnitude(s) of the density modulation(s) (maximum/minimum change of density, thru modification of inter-atomic distances in the wave, relative to the core). The atoms in the shells are shifted from their perfect lattice sites in radial direction according to the defined sign and magnitude of the lattice modification. For the sake of this analysis, we assumed that the starting lattice is that of the corresponding bulk crystal.

The density waves are described by $x(r)$ diagrams, Fig. 1(b), where x gives, in %, the deviation of the local inter-atomic distances r (within a shell of certain thickness and defined distance from the grain center, the wave), from the corresponding distances in the parent perfect structure; x is the distance from the grain center.

The differences in the inter-atomic distances between nanocrystal with a perfect crystal lattice and such a crystal with implemented density waves are described in the form of d plots presenting changes of average global inter-atomic distances resulting from density fluctuations present in the nanograins. These plots, which we calculate for models of nanograins, show characteristic "waves" which reflect their internal structure.

Calculation of theoretical $d(r)$ plots

With introduction of density modulation about each inter-atomic distance r_{i0} observed for a perfect crystal lattice, there appear a number of additional inter-atomic distances. As a result average inter-atomic distances appearing on the $G(r)$ plot for a perfect lattice move to "new" average positions $\langle r \rangle$. In Fig. 1 there is a comparison of four peaks of $G(r)$ calculated for 5 nm diamond grain with the perfect lattice with those with density modulation.

The changes of $\langle r \rangle$ distances within the grain with density modulation waves relative to those of a perfect lattice, r_{i0} are presented in the form of $d(r)$ plot, Fig. 2:

$$d(r) = Dr/r_{i0}; \quad Dr_i = (\langle r \rangle - r_{i0}), \quad (1)$$

where $Dr_i = (\langle r \rangle - r_{i0})$ is the deviation of a given (volume averaged) inter-atomic distance $\langle r \rangle$ from the corresponding r_{i0} distance in the perfect crystal lattice. The r_i values vary between the shortest interatomic distance r_1 , which is the shortest inter-atomic bond in the grain, and the longest distance which, for spherical grains, is the grain diameter $2R$ ($r_1, Er, E2R$).

An alternative interpretation of $d(r)$ plot is that it shows/reflects changes of the apparent lattice parameter $alp(r)$ calculated for individual r -distances relative to the lattice parameter of the parent perfect structure, a_0 :

$$d(r) = Dr/r_{i0} = [1 - alp(r)/a_0]$$

Unique properties of the $d(r)$ plot

The shape of $d(r)$ function depends on relative changes of inter-atomic distances along the grain diameter, and it preserves its shape without regard to specific atomic arrangements of the parent/reference structure. The positions of "waves" appearing on d -plots are determined uniquely by distribution of density waves along the grain diameter. The amplitude of the d -waves depends on the magnitude of density variations about the density of the reference parent structure. The sequence of "waves" appearing on d -diagrams (starting from the shortest distances) is determined by a sequence of density waves emerging from the grain surface towards the grain center, Fig. 3.

Determining experimental $d(r)$ plots

Due to a strong overlap of individual r -distances, only several shortest inter-atomic distances can be determined from experimental $d(r)$ plots. Therefore, it is practical to derive the d diagrams thru $alp(r)$ values using the "real space structure refinement" program, e.g. PDFgui. Individual $alp(r)$ values are determined for specific intervals of r -values of the experimental $G(r)$ plot and the calculated $alp(r)$ values are related to the middle of a given r -interval.

Samples

Two different commercial powders were examined:

UD96 powders:

- A: commercial UD96 powder annealed at 300°C, measured at RT;
- B: sample A additionally purified with a mixture of sulfuric acid/chromic anhydride (RT);
- C: sample A additionally purified with ion-exchange resins, (RT);
- D: sample A additionally purified with ozone, (RT);
- E: sample A after 1h annealing at 1200°C, (RT);
- F: sample D measured at 15K.

UD90 powders:

- A: commercial UD90 powder after annealing at 300°C;
- B-E: sample A after 1 h annealing at 600, 800, 1000, and 1200°C, respectively.

Examples of experimental scattering factor $S(Q)$ and $G(r)$ plots of the samples are given in Fig. 4 and 5.

Neutron diffraction data of diamond nanopowders were collected at NPDF Station, LANSCE at LANL, Los Alamos, USA (project #20062110).

Lattice parameters of nano-diamond

Reciprocal space analysis

Since positions of Bragg reflections measured for nano-diamonds are not mutually correlated, determination of a single, specific value of the lattice parameter for a given sample is practically impossible. Fig. 6 shows "dispersion" of lattice parameters calculated for individual Bragg reflections; the difference between minimum and maximum of lattice parameters calculated for individual reflections is about 0.3% or more.

The specific shape of $alp(Q)$ plots was previously interpreted with reference to a core-shell model and a reasonably good match between experimental and theoretical $alp(Q)$ plots was obtained for a model in which crystalline diamond core was surrounded by a surface shell 5 Å thick, with inter-atomic distances about 5% longer relative to those in the macro-crystalline diamond [1].

Real space analysis

Real space refinement of experimental $G(r)$ plots with application of PDFgui program yields lattice parameters with differences between individual samples by about 0.1% for UD96 and only about 0.05% for UD90 samples, Tables I and II.

Internal structure of nano-crystalline diamond

Experimental $G(r)$ plots of nano-diamonds were elaborated using PDFgui refinement program where lattice parameters were calculated for several Å-wide r -intervals.

Figs. 7-10 show experimental d -plots along with those obtained for models with three density modulation waves present between the grain core and the surface shell, c.f. Fig. 3(d). In Figs. 7-10 the broken lines mark the average lattice parameters as refined for full r -range with the PDFgui program, which are also equal to the average lattice parameters calculated for the corresponding models.

Experiment

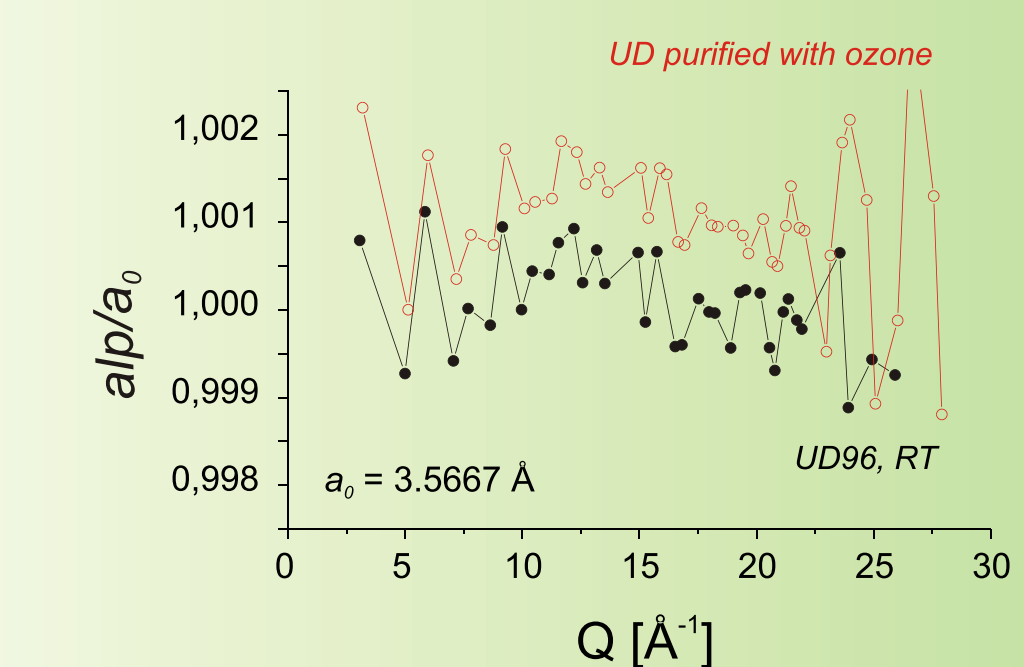


Fig. 6 Relative apparent lattice parameters determined for UD 96 nano-diamond powders.

Table I Lattice parameters of UD96 samples as refined by the PDFgui program

Sample	A	B	C	D	E	F
a	3.5658	3.5687	3.5692	3.5711	3.5649	3.5703
a/a ₀	0.9998	1.0006	1.0007	1.0012	0.9995	1.0010

Table II Lattice parameters of UD90 samples as refined by the PDFgui program

Sample	A	B	C	D	E
a	3.5696	3.56985	3.5697	3.5685	3.5673
a/a ₀	1.0008	1.0009	1.00085	1.0005	1.0004

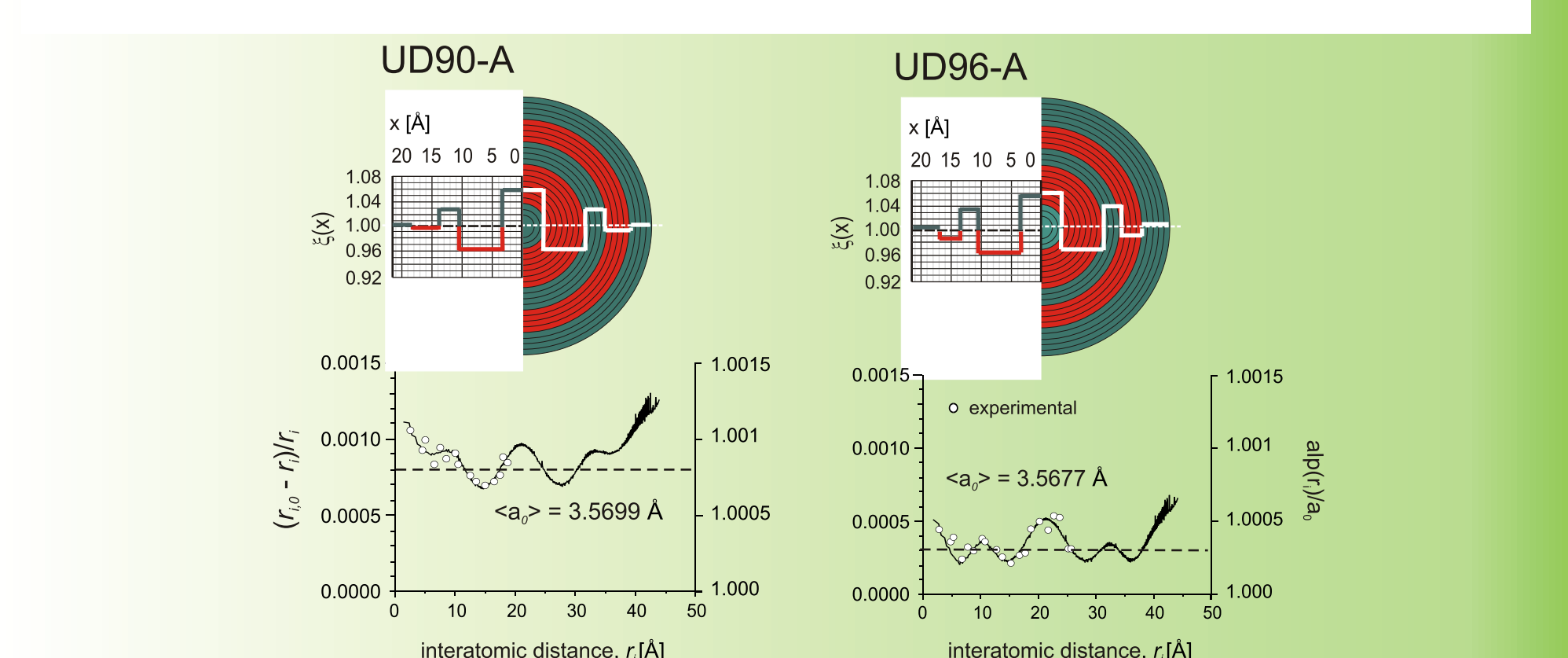


Fig.7 Experimental and theoretical d -plots of UD90 and UD96 nano-diamond powders.

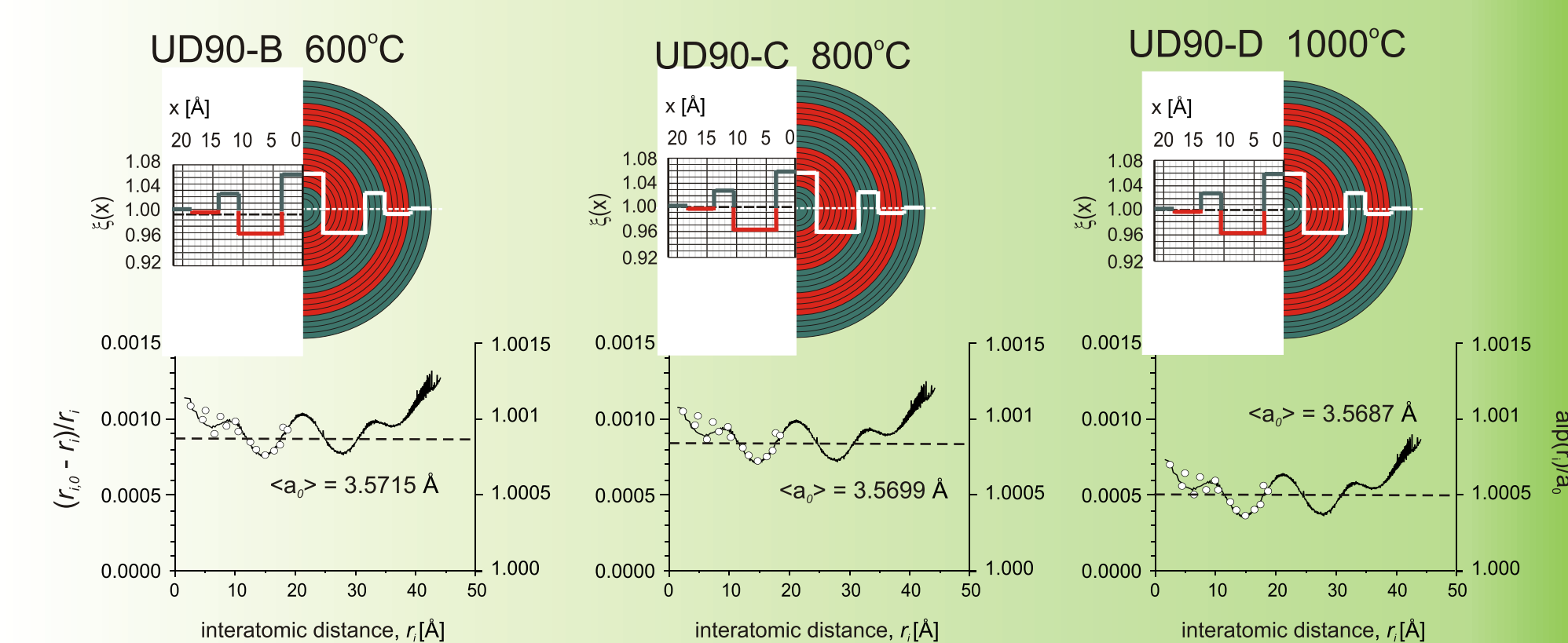


Fig.8 Experimental and theoretical d -plots of UD90 powder annealed at 600, 800, and 1000°C

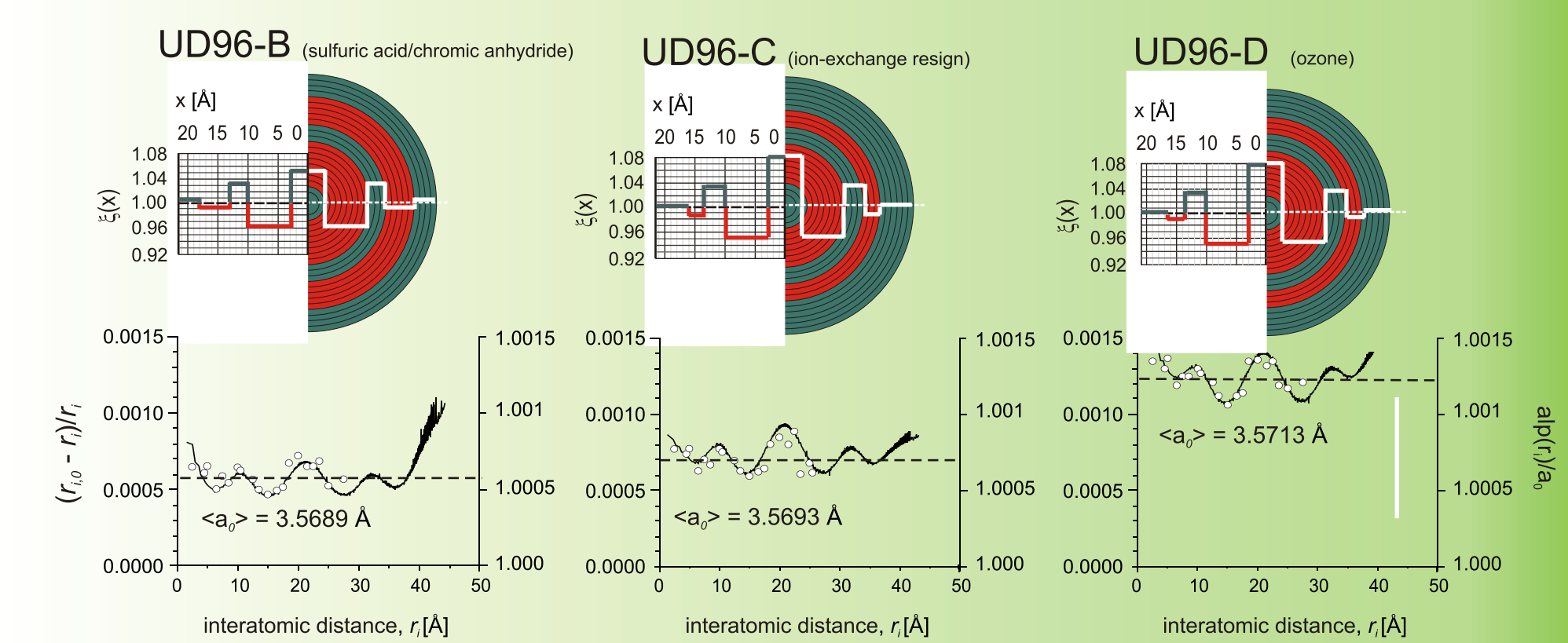


Fig.9 Experimental and theoretical d -plots of UD96 powder after additional cleaning (samples B, C, and D)

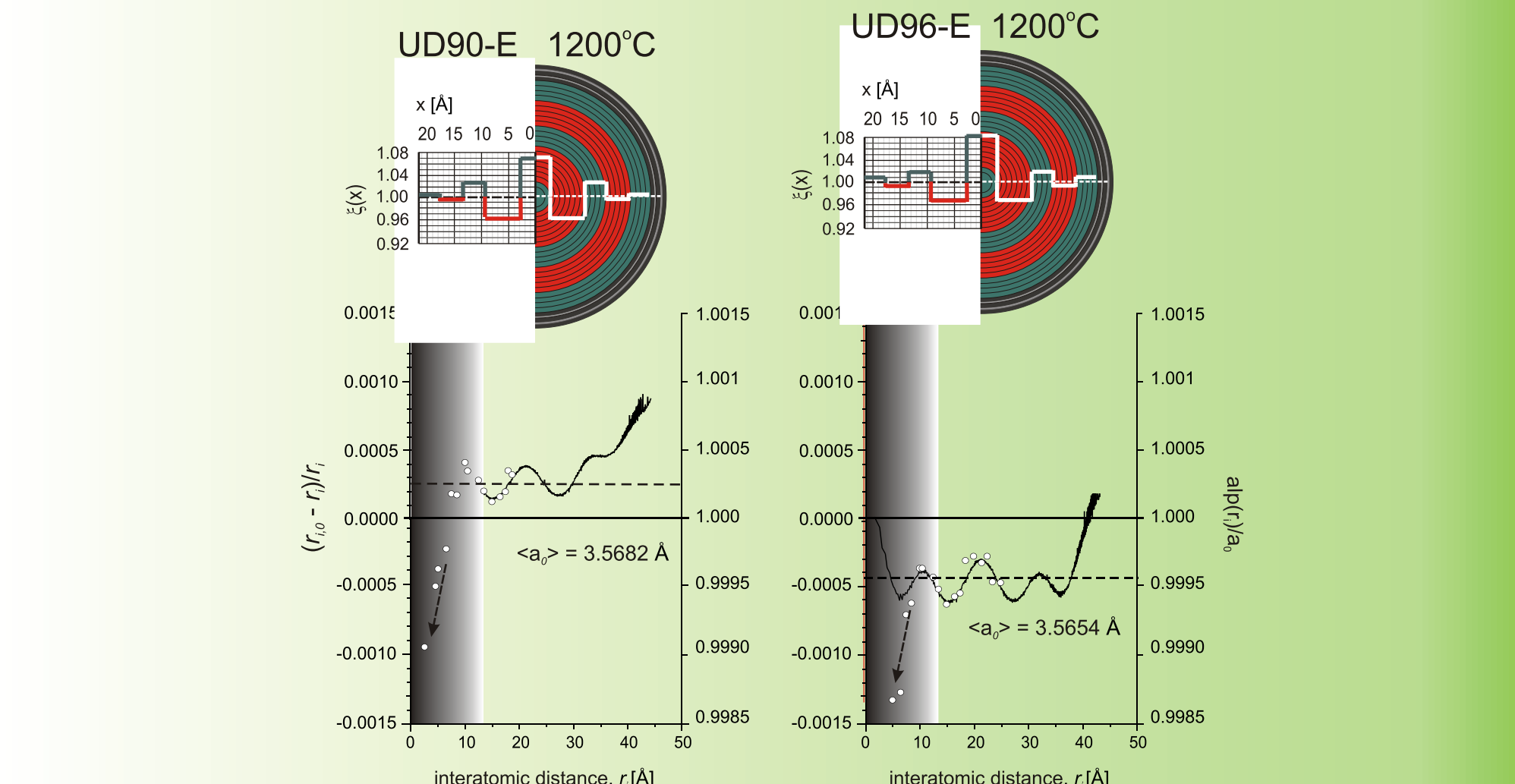


Fig.10 Experimental and theoretical d -plots of UD90 and UD96 powders annealed at 1200°C.

Summary - conclusions

1. All nano-diamond samples show similar density modulation structures with three density waves between the grain core and the surface shell
2. The diameter of diamond nano-grain is about 4.3 nm, except for the powders additionally purified with ozone (sample UD96-D)
3. Additional purification of UD96 with ozone leads to reduction in the thickness of the surface shell (Fig. 10 D), and to an increase in the average lattice parameter.
4. Powders UD90 show thinner surface shell and larger average lattice parameter than powders UD96.
5. Annealing of UD90 powder up to 800°C has no effect on the internal structure of nano-grains.
6. Annealing of diamond nanograins at 1000-1200°C leads to a decrease in the average lattice parameter of the grains, Fig. 11. A much stronger decrease in the lattice parameter is observed in UD96 sample, probably due to a thicker surface layer relative to UD90. Note: For these samples the interatomic distances up to about 10 Å cannot be measured precisely due to a presence of non-diamond carbon covering the diamond nanograins, c.f. Figs. 5 and 6.
7. The observed changes in the inner structure of the nanocrystals of diamond observed after sample treatments could be explained by changes in the graphite-like over-layer covering the diamond-structured part of the nanocrystallite.

[1] B. Palosz, C. Pantea, E. Grzanka, S. Stelmakh, Th. Proffen, T.W. Zerda, W. Palosz, Diamond and Related Materials 15 (2006) 1813-1817 (2006); [2] B. Palosz, S. Stelmakh, E. Grzanka, S. Gierlotka, and W. Palosz, Z. Kristallographie 222 (2006) 580; [3] B. Palosz, E. Grzanka, S. Gierlotka, S. Stelmakh, Z. Kristallographie, 225 (2010) 88; [4] B. Palosz, Denver X-ray Conference Proceedings, *Advances in X-ray Analysis*, Volume 55 (2011); [5] S. Stelmakh, E. Grzanka, S. Gierlotka, and B. Palosz, Denver X-ray Conference Proceedings, *Advances in X-ray Analysis*, Volume 55 (2011).